

See discussions, stats, and author profiles for this publication at: <https://www.researchgate.net/publication/222395015>

# Binding of calcium to phosphatidylcholine–phosphatidylserine membranes

ARTICLE *in* COLLOIDS AND SURFACES A PHYSICOCHEMICAL AND ENGINEERING ASPECTS · JULY 2006

Impact Factor: 2.75 · DOI: 10.1016/j.colsurfa.2005.10.014

---

CITATIONS

60

---

READS

43

3 AUTHORS, INCLUDING:



Rumiana Dimova

Max Planck Institute of Colloids and Interfa...

103 PUBLICATIONS 2,568 CITATIONS

SEE PROFILE

# Binding of calcium to phosphatidylcholine–phosphatidylserine membranes

Cornelia G. Sinn, Markus Antonietti, Rumiana Dimova\*

*Max Planck Institute of Colloids and Interfaces, Am Mühlenberg 1, 14476 Golm, Germany*

Received 14 September 2005; received in revised form 6 October 2005; accepted 7 October 2005

Available online 21 November 2005

Dedicated to Professor Ivan B. Ivanov (LCPE, University of Sofia) on the occasion of his 70th birthday.

## Abstract

We study the adsorption of calcium to charged lipid membranes composed of phosphatidylcholine (PC) – phosphatidylserine (PS) mixtures. An elaborate set of techniques is used to characterize the binding process for varying surface charge of the membrane and carefully chosen experimental conditions. Comparing results obtained from different approaches we aim at unifying and explaining scatter in literature data and giving a coherent picture of the phenomena. The presence of phosphatidylserine in the membrane strongly increases the calcium concentration at the vicinity of the membrane effectively enhancing the binding to the neutral lipid. Calcium binding lowers the surface potential as observed from  $\zeta$ -potential measurements. The isotherms of the adsorption process as measured with isothermal titration calorimetry (ITC) show that the binding process is endothermic, counterintuitively to what is expected for Coulomb interactions. The process is entropy driven and related to liberation of water molecules from the hydration shells of the ion and the lipid headgroups. In addition, the data shows the presence of a second process, apart from binding, which occurs at relatively low calcium concentrations. Differential scanning calorimetry (DSC) measurements in the corresponding concentration interval discards the hypothesis that this process is related to phase separation of lipids in presence of calcium but rather to condensation effect of the calcium ions. Turbidity measurements on vesicle solutions support this observation. Finally, the data suggest that the presence of phosphatidylserine in the bilayers can finely tune the interaction of calcium with lipid membranes and give rise to a spectrum of phenomena strongly dependent on the ion concentration.

© 2005 Elsevier B.V. All rights reserved.

**Keywords:** Vesicles; Model membranes; Calcium binding; Adsorption; Isothermal titration calorimetry; Giant unilamellar vesicles; Ion selective electrode

## 1. Introduction

Calcium ions have an especially important role in many cellular processes [1]. Their specific interaction with biological and model membranes is essential not only for the structure, dynamics, and stability of membranes [2], but also for processes like endo- and exo-cytosis, and for the transport of small molecules across membranes. Membrane fusion, for example, has been shown to be triggered by calcium ions [3,4]. Furthermore, cal-

cium ions are an integral part of signal transduction, and so is their interaction with the neuron membrane [5]. The calcium ions bind naturally to negatively charged phospholipids as phosphatidylserine (PS) [6–9] and phosphatidylglycerol [10,11] but presumably rather weakly to zwitterionic lipids as phosphatidylcholine (PC) [8].

In order to study the binding mechanism of  $\text{Ca}^{2+}$  to PC and PS membranes, a number of techniques have been employed: X-ray diffraction [12,13], calorimetry [4,14–17], NMR [8,18–22], calcium selective electrode [23], IR spectroscopy [24] and particle electrophoresis [14,21,7]. Though some studies have determined the intrinsic binding constants of  $\text{Ca}^{2+}$  to PC, the reported values are rather deviating and scatter between about  $0.1 \text{ M}^{-1}$  and  $100 \text{ M}^{-1}$ . Similar is the situation with data on calcium binding to charged membranes. One of the reasons for the large scatter is that the experiments have been performed at different conditions, e.g. presence or absence of NaCl, various concentration intervals of  $\text{CaCl}_2$ , multilamellar or unilamellar systems, different osmolarity conditions, varied membrane charge and composition.

**Abbreviations:** PC, phosphatidylcholine; PS, phosphatidylserine; DOPC, 1,2-dioleoyl-sn-glycero-3-phosphatidylcholine; DOPS, 1,2-dioleoyl-sn-glycero-3-phosphatidylserine (sodium salt); SOPC, stearoyl-oleoyl-sn-glycero-3-phosphatidylcholine; SOPS, stearoyl-oleoyl-sn-glycero-3-phosphatidylserine (sodium salt); LUV, large unilamellar vesicle; GUV, giant unilamellar vesicle; DSC, differential scanning calorimetry; ITC, isothermal titration calorimetry; ISE, ion selective electrode; DLS, dynamic light scattering

\* Corresponding author. Tel.: +49 331 567 9615; fax: +49 331 567 9612.

E-mail address: [dimova@mpikg.mpg.de](mailto:dimova@mpikg.mpg.de) (R. Dimova).

As we are interested in the details of ion binding to lipid membranes which result only from the quantitative comparison of different techniques, it is the intention of this paper to give a coherent picture and clarify inconsistency between data obtained using various techniques and membrane systems at different conditions or bilayer composition. We use one and the same lipid system under carefully controlled outer ionic strength and osmotic conditions and study it using an elaborated selection of techniques. We prepare unilamellar vesicles of defined size composed of different PC:PS ratio to cover a certain range of membrane charge and characterize the  $\text{Ca}^{2+}$  ion binding with thermodynamic techniques (isothermal titration calorimetry (ITC) and differential scanning calorimetry (DSC)), turbidity and dynamic light scattering (DLS),  $\zeta$ -potential measurements, phase contrast microscopy, and the ion selective electrode (ISE). Throughout these experiments, we will partly resolve the reasons for the rather large scatter of data in the literature and come up with a picture of the mechanisms of ion binding both on charged and uncharged phospholipids membranes.

## 2. Materials and methods

The following section introduces the materials used as well as the extensive set of techniques applied to study the interaction of calcium with the lipid membranes.

### 2.1. Materials

1,2-Dioleoyl-sn-glycero-3-phosphatidylcholine (DOPC) and 1,2-dioleoyl-sn-glycero-3-phosphatidylserine (sodium salt) (DOPS) were purchased from Avanti Polar Lipids Inc. (Birmingham, AL) and used without further purification. In few cases stearyl-oleoyl-sn-glycero-3-phosphatidylcholine (SOPC) and stearyl-oleoyl-sn-glycero-3-phosphatidylserine (sodium salt) (SOPS) were employed (Avanti Polar Lipids Inc.). The lipids were transported from the manufacturer solubilized in chloroform filled into amber borosilicate glass bottles. They were stored at  $-20^\circ\text{C}$  immediately upon arrival.  $\text{CaCl}_2$  was purchased from Merck (Germany) and  $\text{NaCl}$  from Sigma–Aldrich (Germany). All solutions were prepared using deionised water from MilliQ Millipore system with a TOC of less than 15 ppb and a resistivity of  $18\ \Omega\ \text{cm}$ .

### 2.2. Vesicle preparation

As model membranes we used mainly large unilamellar vesicles (LUV) obtained by extrusion. Because studies on such small vesicles ( $\sim 100\ \text{nm}$  in diameter) give indirect evidence of the interactions occurring, we also examined the membrane behavior directly with microscopy observations. The membranes used in this latter case were giant unilamellar vesicles (GUV).

For the preparation of LUVs, the lipid solution in chloroform was transferred into round-bottom flasks, and the organic solvent was removed by rotary evaporation followed by overnight vacuum pumping. The lipid film was then dissolved in  $\text{NaCl}$  solution (at concentration of  $10\ \text{mM}$  if not mentioned otherwise) by vortexing for about 2 min. LUVs were obtained by

extrusion with LiposoFast™ pneumatic extruder (Avestin Inc., Ottawa, Canada), under nitrogen gas at a pressure of  $200\ \text{kPa}$ . The final lipid concentrations were ranging between  $10\ \text{mM}$  and  $40\ \text{mM}$ . The extrusion was performed in three stages, first 31 times through a  $200\text{-nm}$  diameter pore polycarbonate filter, then 21 times through a  $100\text{-nm}$  diameter pore filter and finally 41 times through a  $50\text{-nm}$  diameter pore filter. Vesicles prepared in this way generally have a narrow size distribution as confirmed with dynamic light scattering and are known to be almost entirely unilamellar [25].

GUVs were prepared by the method of spontaneous swelling as described previously [26] (for details see reference [27]). Briefly, a few drops of the lipid solution in chloroform were spread on a roughened Teflon plate and dried under vacuum. The sample was prehydrated and swollen in  $0.2\ \text{M}$  sucrose solution with  $10\ \text{mM}$   $\text{NaCl}$  and then resuspended in isoosmolar glucose solution with  $10\ \text{mM}$   $\text{NaCl}$ . The purpose of the resulting glucose/sucrose asymmetry across the membrane is to increase the optical contrast due to the difference of the refractive index of the two solutions. The observations were performed in phase contrast mode using an inverted microscope Axiovert 135, Zeiss, Germany equipped with  $40\times$  objective.

### 2.3. Experimental methods

The size of the LUVs was determined with dynamic light scattering, and phase separation of the lipids was investigated using differential scanning calorimetry. Isothermal titration calorimetry and  $\text{Ca}^{2+}$  ion selective electrode were used to characterize the isotherm of calcium binding to membranes. Aggregation of the vesicles and density changes in the solutions were investigated with turbidity measurements. The membrane charge was characterized by  $\zeta$ -potential measurements.

#### 2.3.1. Dynamic light scattering

Size distribution measurements were performed with an ALV-NIBS High Performance Particle Sizer (ALV-Laser GmbH, Langen, Germany). The instrument uses a  $2\ \text{mW}$  HeNe laser at a wavelength of  $632.8\ \text{nm}$  and detects the scattered light at an angle of  $173^\circ$ . All measurements were performed in a temperature-controlled chamber at  $25^\circ\text{C}$ . The autocorrelation function was measured using exponential spacing of the correlation time. The data analyses were performed with software provided by ALV. The intensity weighted size distribution was obtained by fitting data with a discrete Laplace inversion routine.

#### 2.3.2. Isothermal titration calorimetry

ITC measurements were performed with a VP-ITC microcalorimeter from MicroCal Inc. (Northampton, MA). The working cell ( $1.442\ \text{ml}$  in volume) was filled with the LUV solution and the reference cell with  $10\ \text{mM}$   $\text{NaCl}$  solution (no difference in the measurements was observed when the reference cell was filled with pure water). Ten microliters aliquots of  $\text{CaCl}_2$  solution were injected stepwise into the working cell filled with vesicle suspension or solvent only. All samples were degassed shortly before performing the measurements. The sample cell

was constantly stirred at a rate of 310 rpm, and the measurements were performed at 25 °C. The data analyses were carried out with Origin software provided by MicroCal.

### 2.3.3. $\text{Ca}^{2+}$ ion selective electrode

Binding isotherms were measured using a  $\text{Ca}^{2+}$  ISE from Mettler Toledo, Switzerland. The electrode measures the potential difference between a solution and a reference electrode. This potential difference is proportional to the logarithm of the  $\text{Ca}^{2+}$  concentration in the solution. The calibration of the electrode was carried out with solutions of  $\text{CaCl}_2$  with concentrations ranging from 1  $\mu\text{M}$  to 5 mM. The calibration curves were subsequently used to determine the concentration of free calcium in the vesicle solutions.

### 2.3.4. Turbidity measurements

Solution turbidity was measured with a UV–vis spectrophotometer Helios Gamma (Thermo Spectronic, UK). Aggregation effects were investigated by injecting small aliquots of  $\text{CaCl}_2$  solution into the LUV suspension and measuring the absorbance at the wavelength of maximal absorption (wavelength scans were previously measured). The decrease in absorbance due to dilution was determined as well, by injecting NaCl solution into the vesicle suspensions.

### 2.3.5. Differential scanning calorimetry

The instrument used in this work is a VP-DSC microcalorimeter from MicroCal (Northampton, MA). The lipid concentration of solutions used for the DSC measurements was 1 mg/ml and the samples were examined at a scanning rate of 30 K/h by applying two heating and two cooling cycles between 2 °C and 22 °C. Baseline subtraction was performed using the MicroCal Origin software. The influence of calcium on the phase separation of PS/PC (2:8) LUVs was studied by adding calcium to the vesicle solution yielding the desired molar ratios of  $\text{Ca}^{2+}$  to lipid.

### 2.3.6. $\zeta$ -potential measurements

Electrophoretic mobility of the vesicles was measured using a Malvern Zetasizer 3000 HS (Malvern Instruments Ltd., UK). The mobility  $u$  was converted to  $\zeta$ -potential using the Helmholtz–Smoluchowski relation  $\zeta = u\eta/\epsilon\epsilon_0$ , where  $\eta$  is the solution viscosity;  $\epsilon$ , the dielectric constant of water and  $\epsilon_0$ , the permittivity of free space.

## 3. State of the art

There is an abundance of studies on adsorption of  $\text{Ca}^{2+}$  on phosphatidylcholine membranes. In most of the early works a 1:1 interaction of Ca to PC was considered. Seelig and co-workers [20,28] have studied  $\text{Ca}^{2+}$  adsorption to PC membranes, exploring a large interval of  $\text{CaCl}_2$  concentrations. Comparison of different binding models (Langmuir adsorption, 1:1, 1:2 and 1:3 stoichiometry interactions) revealed that the interaction at elevated calcium concentrations is best described with formation of a ternary complex of  $\text{Ca}^{2+}$  to phospholipids in 1:2 ratio. It is edifying to remind that at low calcium concentrations (bound

calcium  $\ll$  lipid concentration) the models converge to simple nonspecific 1:1 partitioning, also known as Henry–Dalton binding:  $X_{\text{Ca}} = KC_{\text{Ca}}^{\text{S}}$ . Here, the ratio of moles bound calcium per moles lipid,  $X_{\text{Ca}}$  is proportional to the concentration of calcium in the vicinity of the membrane,  $C_{\text{Ca}}^{\text{S}}$ . The proportionality factor  $K$  is the binding equilibrium constant and is in units  $\text{M}^{-1}$ . Indeed, a later study [29] based on  $\zeta$ -potential measurements of vesicles in a large range of calcium concentrations showed that the 1:1 model interprets the obtained data better. The ambiguity in the interaction stoichiometry has been also addressed by simulation studies and recently [30] it has been shown that the binding of calcium to PC membranes proceeds in a multistep mechanism leading to even higher coordination (1:4) of lipids by the ions.

Whatever the molecular stoichiometry of the interaction, it is instructive to mention here that for the elaboration of a model on the binding of  $\text{Ca}^{2+}$  to membranes, the ion distribution near a lipid bilayer has to be carefully considered. This is particularly important for multicomponent membranes containing charged lipids. Every membrane, depending on its composition, is characterized by a certain surface potential,  $\psi_0$ . An approximate experimental quantification of  $\psi_0$  can be obtained from electrophoretic measurements of the zeta potential,  $\zeta$ , of the vesicles in solution [21,14]. The relation between the concentration of a certain ion  $i$  close to a membrane,  $C_i^{\text{S}}$ , and its concentration in the bulk,  $C_i^{\text{B}}$ , can be approximated by the Boltzmann equation  $C_i^{\text{S}} = C_i^{\text{B}} \exp(-z_i F\psi_0/RT)$  where  $z_i$ , is the ion charge;  $F$ , the Faraday's constant;  $R$ , the gas constant; and  $T$ , the absolute temperature. The exponential factor in the equation can be considered as an 'activity' correction since it yields the concentration of the thermodynamically active ions at the membrane surface. Therefore, all binding models which consider the equilibrium between the ions in solution and ions bound to a membrane must necessarily take into account the active or effective concentration of ions taking part in the interaction, i.e.  $C_i^{\text{S}}$  and not  $C_i^{\text{B}}$ . This correction becomes essential for membranes containing charged lipids where the surface concentration of calcium can be enhanced by at least two orders of magnitude [28] with respect to the bulk concentration. The surface potential of such membranes results in membrane charge,  $\sigma$ , which can be estimated [31] from the Gouy–Chapman theory  $\sigma^2 = 2000\epsilon\epsilon_0 RT \sum_i C_i^{\text{B}} [\exp(-z_i F\psi_0/RT) - 1]$ , where  $\epsilon = 78$

is the dielectric constant of water (at 25 °C) and  $\epsilon_0$  is the permittivity of free space. The summation is over all the ions in the solution. On the other hand, according to the Graham equation  $\sigma = (\epsilon\epsilon_0\zeta)/(\kappa_{\text{D}})$ , where  $\kappa_{\text{D}}$  is the Debye length. Knowing the surface charge of the membrane and combining the Boltzmann and Gouy–Chapman equations with the mass conservation condition one can estimate the surface concentration of the ions. Using this approach several groups have been able to characterize calcium binding to neutral (PC) [29] and charged (PS) [7] membranes on the bases of  $\zeta$ -potential measurements.

It is important for the discussion below to mention that the interaction of calcium with PC membranes was already reported to be associated with dehydration of the lipids. Infrared spectroscopy data suggested deep penetration of divalent ions in the

polar region of the bilayer leading to partial dehydration of the headgroups [24]. The authors speculate that this is due to partial dehydration of the calcium ions and interaction with the hydration shells of the lipid headgroups.

## 4. Results

### 4.1. Enthalpy of calcium binding and competition with sodium ions

The main object of this work is to study binding of calcium to membranes of different surface charge. We approach this problem using isothermal titration calorimetry. In this work, we present a set of experiments where the surface charge of the membrane was set by the DOPS content at the following PS:PC molar ratios  $\gamma_{PS} = 0, 0.11, 0.2$  and  $0.25$  (higher PS fractions were not explored because of possible lipid demixing [32,12]).

Before commencing ITC measurements on small unilamellar vesicles the following problem has to be carefully considered. When an aqueous solution of lipid vesicles is mixed with a salt solution, the vesicles become subject to osmotic shock. This asymmetry across the lipid bilayer can give yield to an additional signal in calorimetry measurements [33] and thus lead to ambiguity in the interpretation of the signal as due to calcium-lipid binding, only. A way to avoid osmotic effects is to extrude the vesicles in NaCl solution and titrate them with isoosmolar  $\text{CaCl}_2$  solutions.

In addition, at physiological conditions the interaction of calcium with biological membranes naturally occurs in presence of salts, e.g. NaCl. Typical intracellular concentrations are on the order of 15 mM [5]. However, studying calcium adsorption in presence of NaCl leads to some complexity as sodium ions may compete with calcium for binding to the lipid headgroups even though with low affinity (see e.g. [34,35]). The presence of NaCl has screening effect on the membrane surface charge which leads to a decrease in the enrichment of  $\text{Ca}^{2+}$  near the membrane (see previous section) and consecutively, results in a decrease of the binding at the membrane: an increase in the NaCl concentration by a factor of 10 was reported to reduce the concentration of bound  $\text{Ca}^{2+}$  by a factor of 100 [36]. Lower calcium binding in titration calorimetry translates into lower heat signal and leads to difficulties in performing reliable ITC experiments.

Thus, one faces the following constraint: the vesicle solution has to be prepared in NaCl in order to avoid osmotic effects, but the NaCl concentration should not be very high so that calcium binding is not screened to the extend of producing a very weak heat signal. To determine an optimum concentration of NaCl in terms of maximum binding and detectable ITC heat signal, titration experiments were performed where vesicle solutions extruded in 100 mM NaCl, 10 mM NaCl and water solutions were titrated with isoosmolar 7 mM  $\text{CaCl}_2$  solutions, as presented in Fig. 1 (in the case of the vesicles extruded in 100 mM NaCl, the osmolarity of the 7 mM  $\text{CaCl}_2$  solution was adjusted by adding NaCl). The heat obtained from reference measurements (simple dilution) where the calcium solutions were injected in vesicle-free NaCl solutions was subtracted. As expected, at high concentration of NaCl the signal approaches

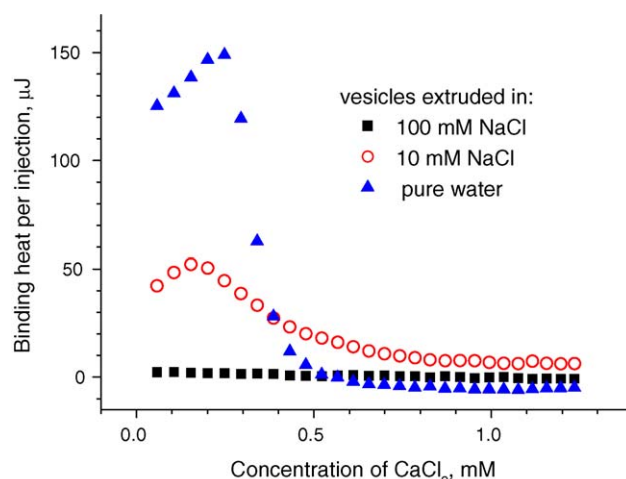


Fig. 1. Binding heat from titrating 10  $\mu\text{L}$  aliquots of 7 mM  $\text{CaCl}_2$  into 8 mM DOPS/DOPC ( $\gamma_{PS} = 0.2$ ) LUV solutions extruded in absence or presence of NaCl at various concentrations (see legend). The binding heat was determined by subtracting the heat of injecting the  $\text{CaCl}_2$  solutions in the respective NaCl solutions or water (the heat of dilution of the vesicles is negligible).

the instrument noise. For comparison we have plotted also a measurement on vesicles extruded in water, where osmotic effects due to the addition of  $\text{CaCl}_2$  are expected [33].

The optimum NaCl concentration for our further measurements was chosen to be 10 mM, corresponding to an isoosmolar solution of  $\text{CaCl}_2$  of 7 mM.

### 4.2. Change in the membrane surface charge due to $\text{Ca}^{2+}$ binding

To determine electrostatic effects on ion binding, electrophoresis measurement were performed. Binding of  $\text{Ca}^{2+}$  to the interface of the PS/PC membrane increases the vesicles surface potential. Knowledge about the vesicles surface charge as a function of added  $\text{Ca}^{2+}$  concentration can, therefore, provide information about the extent of  $\text{Ca}^{2+}$  binding. Electrophoresis does not reveal the direct surface potential, but the electrical potential at the shear plane ( $\sim 2 \text{ \AA}$ ), i.e. the  $\zeta$ -potential. The latter however can be used as an approximate quantification of the surface potential of the vesicles in solution [21,14].

Due to the zwitterionic character of the DOPC headgroups, the  $\zeta$ -potential of a pure DOPC LUVs solution is close to zero, as measured by electrophoresis. The incorporation of negatively charged PS into the membrane decreases the  $\zeta$ -potential leading to negative values. If  $\text{Ca}^{2+}$  is added to the negatively charged vesicle solution, the ions bind to the membrane, and the negative charges of the PS headgroups are compensated by the bound divalent cations. As a consequence, increasing the divalent cation concentration may reverse the sign of the  $\zeta$ -potential for PS vesicles. Using electrophoresis (results shown in Table 1) we observed that the  $\zeta$ -potential changes from  $-42 \text{ mV}$  for a 10 mM DOPS/DOPC,  $\gamma_{PS} = 0.2$ , LUVs in NaCl solution to  $-35 \text{ mV}$  at a calcium concentration of 1.25 mM (corresponding to the final concentration in the ITC experiments, see Fig. 1). The change in the  $\zeta$ -potential is, therefore,  $\Delta\zeta \approx 7 \text{ mV}$ , indicating that  $\text{Ca}^{2+}$  binds to the negatively charged PS/PC membrane.



Table 1

Surface charge ( $\zeta$ -potential) of pure DOPC and DOPS/DOPC ( $\gamma_{\text{PS}} = 0, 0.2$ ) vesicles in 10 mM NaCl measured at various concentration of  $\text{CaCl}_2$ . The accuracy of all the values of the  $\zeta$ -potential is  $\pm 3$  mV

$\text{Ca}^{2+}$ (mM)	$\gamma_{\text{PS}}$	
	0	0.2
0	3 mV	−42 mV
1.25	2 mV	−35 mV
40	12 mV	–

If we want to compare these findings to the binding of  $\text{Ca}^{2+}$  to pure DOPC, we have to take into account that the concentration of the ion at the surface of the PS/PC membrane is increased by the presence of the negatively charged phosphatidylserine and thus the effective concentration of calcium available for binding to the PC in this case is elevated. As discussed in Section 3, the  $\text{Ca}^{2+}$  surface concentration,  $\text{Ca}_s^{2+}$ , can be estimated using the Boltzmann distribution where the surface potential is obtained from the Gouy–Chapmann theory taking into account the corresponding Debye length in the solution (see e.g. [14]). For the PS/PC membranes with 20% surface charge in 10 mM NaCl at a bulk  $\text{Ca}^{2+}$  concentration of 1.25 mM the calcium surface concentration is calculated to be 33 times higher, i.e.  $\text{Ca}_s^{2+} \approx 40$  mM. Consequently, electrophoresis measurements for pure DOPC were performed at this concentration (corresponding to  $\text{Ca}_s^{2+}$  for the PS/PC mixture). We find that the  $\zeta$ -potential changes from 3 mV in the case of pure DOPC to 12 mV for  $\text{Ca}_s^{2+}$  of 40 mM yielding a net  $\zeta$ -potential change of  $\Delta\zeta \approx 9$  mV. Within the experimental error ( $\pm 3$  mV) this value is equal to the one measured for the mixed PS/PC ( $\gamma_{\text{PS}} = 0.2$ ) membrane.

We have to conclude, that the main reason for an enhanced binding of  $\text{Ca}^{2+}$  to mixed PS/PC compared to pure PC membranes is an increased local concentration at the vicinity of the lipid bilayer due to the presence of charge in the bilayer and not due to preferential binding of calcium to phosphatidylserine.

#### 4.3. Effect of surface charge on the $\text{Ca}^{2+}$ binding isotherm

To investigate the influence of surface charge density on the calcium-binding isotherm we performed the titration of 7 mM  $\text{CaCl}_2$  into pure DOPC and into DOPS/DOPC vesicles solutions with various PS mole fractions. Fig. 2 presents the measured binding heats normalized by the moles of added  $\text{Ca}^{2+}$  as a function of  $[\text{Ca}_A^{2+}]/[\text{lipid}_{\text{out}}]$ . Here  $[\text{Ca}_A^{2+}]$  is the concentration of added  $\text{Ca}^{2+}$  and  $[\text{lipid}_{\text{out}}]$  is the total concentration of lipid in the external leaflets of the vesicle membranes (i.e. the lipid accessible for calcium adsorption). The measurement for  $\gamma_{\text{PS}} = 0.2$  is identical to the one displayed in Fig. 1. The error bars represent data deviation averaged over three experiments. The arrows indicate the point where the ratio of added  $\text{Ca}^{2+}$  to PS at the external vesicle monolayers approaches one. Again the heat of dilution of  $\text{CaCl}_2$  which is an exothermic process was separately measured and subtracted before plotting the data in Fig. 2.

In the case of pure DOPC, the binding enthalpy remains slightly endothermic and constant within the error of the measurement, but nonzero throughout the whole titration. Obviously,

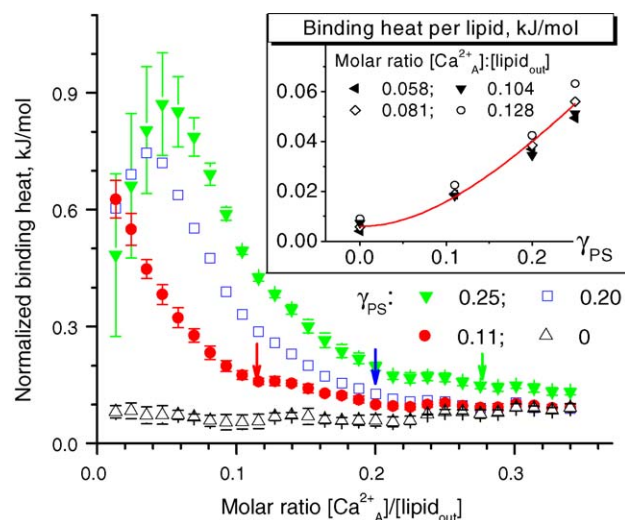


Fig. 2. Molar binding heat for DOPS/DOPC vesicles in 10 mM NaCl with PS fractions  $\gamma_{\text{PS}}$  of 0, 0.11, 0.2 and 0.25 (see legend). The heat is normalized by the moles of added  $\text{Ca}^{2+}$ . Arrows indicate the point where the ratio of added  $\text{Ca}^{2+}$  to PS in the external leaflet of the vesicle membrane approaches one. The inset shows the binding heat normalized by the moles of lipid as a function of mole fraction PS at four molar ratios  $[\text{Ca}_A^{2+}]/[\text{lipid}_{\text{out}}]$  as indicated. The solid line is a fit to the data (see text for details).

binding of  $\text{Ca}^{2+}$  to PC is not saturated at the end of the ITC experiment, where the ratio of  $[\text{Ca}_A^{2+}]$  to  $[\text{lipid}_{\text{out}}]$  is 0.34. This confirms the general observation that divalent cations also adsorb to the zwitterionic phosphatidylcholine (PC) with ion-to-lipid stoichiometries of 1:1 to 1:3 [37].

The data on mixed membranes shows that the increase in surface charge fraction leads to an increase of the endothermic character of the binding heat. In other words, the higher the charge of the membrane is, the more endothermic the binding becomes. This is somewhat counterintuitive, but in good agreement with studies on the binding of alkaline earth cations to phosphatidylglycerol dispersions [38] and binding of  $\text{Ca}^{2+}$  and  $\text{La}^{3+}$  to lipid vesicles [15]. The latter processes were also reported as endothermic. It is interesting to note that the behavior of charged membranes is also very similar to the binding of  $\text{Ca}^{2+}$  onto charged polyelectrolytes [39]. The latter work quantitatively delineates that the ion binding is not due to Coulomb forces, but entropy driven. Thus, the binding of  $\text{Ca}^{2+}$  to the lipid bilayer must also be entropy driven. The molecular origin of this entropy gain is a release of water molecules from the surface hydration layer of the lipid membrane and the dehydration of the  $\text{Ca}^{2+}$  ion upon binding. Indeed, as the endothermic signal is of the order of  $1/3 k_B T$ , where  $k_B T$  is the thermal energy, already the liberation of a few water molecules per head group (2–4) throughout binding is sufficient to explain the scatter in the values of binding constants reported in literature.

With increasing concentration of added calcium, the binding heats of all of the charged vesicles approach the value of pure DOPC. Thus, we assume that in the case of the charged vesicles, the  $\text{Ca}^{2+}$  ions initially mainly interact with the negatively charged PS lipids. When these groups are fully occupied, the ions continue to bind to the neutral PC headgroups. This interpretation is supported by the fact that the ions bind to the vesicles

well beyond  $\text{Ca}^{2+}$  to PS ratios of 1:1 (ion-to-lipid stoichiometries of divalent ions binding to PS membranes are reported to be 1:1 and 1:2 [37,36]). A preferential interaction of cations with negatively charged components in a mixture has been previously proposed [40,41], but has to be considered in the light of the additional electrostatic enrichment effect.

Another concept reported in literature is that the affinity of anionic PS bilayers for  $\text{Ca}^{2+}$  is suppressed as the membrane surface charge density is decreased upon incorporation of the zwitterionic lipid PC [36]. Our data can be used to test this view. In the inset in Fig. 2, we plotted the binding heat normalized over the total moles of lipid as a function of mole fraction DOPS for four different molar ratios  $[\text{Ca}_A^{2+}]/[\text{lipid}_{\text{out}}]$ . As the inset demonstrates, this normalized heat for all four molar ratios collapses to a unique ‘master curve’, which shows an increase with the mole fraction of PS. This behavior is consistent with the one deduced from the  $\zeta$ -potential measurements, e.g. it shows that the membrane charge, i.e. the incorporation of DOPS, mainly effectively changes the surface concentration of  $\text{Ca}^{2+}$ , whereas the binding of  $\text{Ca}^{2+}$  to DOPS and DOPC is essentially the same. This idea is additionally confirmed by a simple model describing the data (solid line) which assumes a linear superposition of the heat from  $\text{Ca}^{2+}$  binding to PC and to PS is assumed. The two contributions are corrected by the molar fractions of each of the components (PC or PS), while the molar enthalpies,  $\Delta H_{\text{PC}}$  and  $\Delta H_{\text{PS}}$  are assumed constant. Thus for the conditions of the measurement (10 mM NaCl concentration, 100 nm vesicle size) we obtain  $\Delta H_{\text{PC}} = 0.006 \pm 0.001$  kJ/mol and for  $\Delta H_{\text{PS}} = 1.26 \pm 0.04$  kJ/mol.

The arrows in Fig. 2 indicate the points where the added calcium corresponds to the concentration PS in the external leaflets of the vesicles in the solution. As expected, after this point of 1:1  $\text{Ca}^{2+}$ :PS the binding signal approaches the signal from calcium binding to pure PC (open triangles).

Fig. 2 presents an additional feature of the binding isotherm, which we have not discussed yet. In particular, at PS:PC mole ratios of 0.2 and 0.25 a maximum in the binding heat appears. It shifts to higher concentrations of added  $\text{Ca}^{2+}$  with increasing PS mole fraction. This maximum in the overall endothermic binding process can be indicative for a secondary exothermic process taking place at low  $[\text{Ca}_A^{2+}]/[\text{lipid}_{\text{out}}]$  ratios. For example, such process could be fusion or aggregation of vesicles, or calcium induced phase separation of the lipid mixtures. We address this issue using differential scanning calorimetry and spectrophotometry, as discussed below.

Differential scanning calorimetry was applied to study the influence of calcium binding on the thermal phase transition of PS/PC vesicles. Calorimetry data can provide evidence for the hydration/dehydration effects of the lipids upon ion binding. The phase transitions of DOPC and DOPS from the ordered gel phase to the disordered liquid-crystalline phase are reported in the literature to occur at  $-17^\circ\text{C}$  [42] and  $-11^\circ\text{C}$  [43], respectively. The phase transition of a homogeneous lipid mixture is expected to lie in between these values. The DSC experiments on vesicle solutions are restricted to temperatures above the freezing point of water. Hence, instead of with DOPC/DOPS we chose to work with another PC/PS couple, in particular SOPC and SOPS

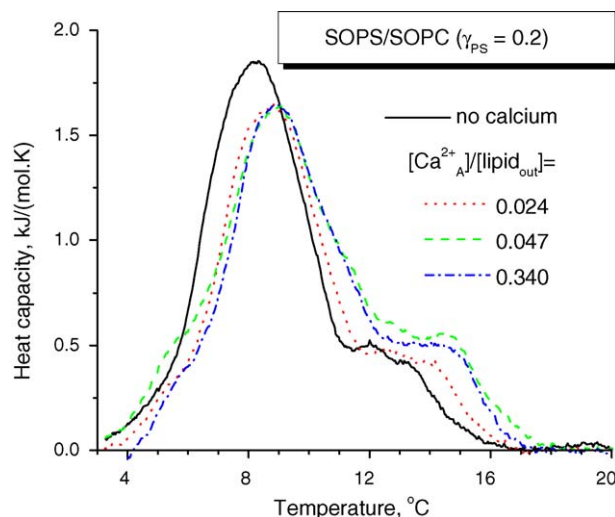


Fig. 3. DSC heating curves of SOPS:SOPC ( $\gamma_{\text{PS}} = 0.2$ ) LUVs in 10 mM NaCl with increasing amounts of added  $\text{CaCl}_2$  (see legend for the molar ratio of added  $\text{Ca}^{2+}$  to total lipid concentration).

whose gel to liquid crystal phase transitions are above this temperature ( $5.5^\circ\text{C}$ , data not shown, and  $17^\circ\text{C}$  [44], respectively). The only structural difference between the pairs SOPC/SOPS and DOPC/DOPS is that the latter have two unsaturated chains whereas the former have only one unsaturated chain. The head-groups which are most essential for  $\text{Ca}^{2+}$  binding are identical for both couples.

The specific heat capacity of the SOPS/SOPC ( $\gamma_{\text{PS}} = 0.2$ ) LUVs solution with increasing amounts of added  $\text{CaCl}_2$  is shown in Fig. 3. The lipid mixture in absence of  $\text{Ca}^{2+}$  shows two endothermic phase transitions. This is indicative for the existence of two phases. In particular, the peak at  $7.5^\circ\text{C}$  and the weaker one at  $12.5^\circ\text{C}$  can be assigned to PC and PS enriched phases, respectively. Thus, at  $\gamma_{\text{PS}} = 0.2$  partial phase separation occurs. Increasing amounts of SOPS in the membrane, e.g. to  $\gamma_{\text{PS}} = 0.25$ , presumably leads to enhancing the phase separation, and vice versa, for a lower PS fraction, e.g.  $\gamma_{\text{PS}} = 0.11$ , we speculate that this effect is less pronounced.

We consider now the measurements performed in presence of calcium. The calcium concentrations were selected so that concentrations both below and above the maximum observed in the ITC measurements (see the curve for  $\gamma_{\text{PS}} = 0.2$  in Fig. 2) are probed. Interestingly, both of the phase transition peaks shift to higher temperatures, without changing the relative integrals significantly. This shift suggests that the presence of  $\text{Ca}^{2+}$  induces structural changes either of the hydrocarbon chain packing or of the polar head group packing, e.g. inducing changes of the hydration shell, which is well known for the binding of divalent cations to negatively charged membranes. Both peaks, indicative for SOPC and SOPS enriched phases, shift by about 1 K and maximum 4 K, respectively. The shifts occur at lower calcium concentrations (before the ITC maximum) while the further addition of calcium does not effectively change the data (compare the curves for the two highest ratios).

Since the observed phase transitions are shifted to higher temperatures, the packing of the lipids in the presence of  $\text{Ca}^{2+}$

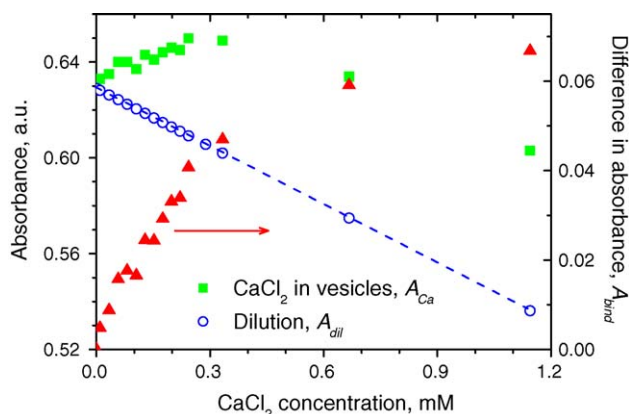


Fig. 4. Turbidity measurements. Absorbance at 350 nm (left axis) of 8 mM DOPS/DOPC ( $\gamma_{PS}=0.2$ ) LUVs upon titration with small aliquots of 7 mM  $\text{CaCl}_2$  (filled squares) and with 10 mM NaCl (open circles). The difference of the two signals (filled triangles, right axis as indicated by the arrow) is the absorbance associated with the interaction of  $\text{Ca}^{2+}$  with the lipid bilayer (see text for details).

is energetically more stable. These results are in agreement with previous measurements where the endothermic transition of PS is shifted to higher temperatures due to the addition of  $\text{Ca}^{2+}$  [16,45]. The DSC data indicate that this stabilization occurs similarly for both PC- and PS-rich phases indicating that ion binding or immobilization is very similar.  $\text{Ca}^{2+}$  definitely does not only bind to the charged PS but comparably to the zwitterionic PC headgroups. The shift in the phase transition due to  $\text{Ca}^{2+}$  binding is only observed up to ion-to-lipid ratios corresponding to the ITC maximum, which is well below (at least a factor of 6) the absolute binding capacity of the membranes. This means that the first few  $\text{Ca}^{2+}$  ions bound promote the structural membrane changes, whereas further dehydration by added  $\text{Ca}^{2+}$  leaves the structure of the membrane essentially unaltered.

Spectrophotometry is a technique which is very sensitive to structural changes and aggregation effects in vesicle dispersions. Thus, the absorbance of a PS/PC vesicle solution was studied as a function of added  $\text{Ca}^{2+}$ . Fig. 4 shows the change in the absorbance at 350 nm,  $A_{Ca}$ , of 8 mM vesicle suspension DOPS/DOPC ( $\gamma_{PS}=0.2$ ) following the stepwise addition of 7 mM  $\text{CaCl}_2$  solution. The signal due to dilution of the vesicle solution,  $A_{dil}$ , was determined in a separate experiment by addition of the same aliquots of 10 mM NaCl solution to the vesicle solution. The change in the absorbance associated with the calcium binding only,  $A_{bind}$ , was then calculated from the dif-

ference  $A_{bind} = A_{Ca} - A_{dil}$  as plotted in Fig. 4 (right ordinate). As the measurements demonstrate, the optical contrast or scattering power of the vesicles increases upon the addition of  $\text{CaCl}_2$ . Simultaneously, for each solution we measured the vesicle size distribution using DLS (data not shown). Within the instrument error no increase in the particle mean size was observed, thus we rule out the possibility that the turbidity changes are due to aggregation. Instead we conclude that the membranes undergo local increase of optical density. The latter is obviously due to the adsorption of  $\text{Ca}^{2+}$  on the lipids, as observed in the above-described ITC and DSC measurements. With increasing  $\text{Ca}^{2+}$  concentrations, the binding absorbance (right axis) approaches a plateau indicating the proximity of saturation of the binding. It is to be noted that the final points of these measurements were generated at molar  $\text{Ca}^{2+}$  to PS ratios of 1.5 that is well beyond a molar stoichiometry or a balance of charges. Obviously, such lipid bilayers can trap  $\text{Ca}^{2+}$  very efficiently to an extent which is well beyond a molecular binding picture. This is important in the context of biomineralization, where nucleation of  $\text{Ca}^{2+}$ -salts under the geometric and physico-chemical control of vesicles is a well-known principle [46].

#### 4.4. Microscopic effects of calcium binding on vesicles

Using ITC, DSC, DLS and turbidity measurements we characterize the changes occurring at molecular and nanometer scale upon the binding of calcium. All of these techniques indirectly characterize the process. To directly examine the structural consequences of  $\text{Ca}^{2+}$  binding on the micron scale, we used giant vesicles observed with phase contrast microscopy to monitor the changes of a single vesicle upon the binding of  $\text{Ca}^{2+}$ . We studied vesicles of DOPS/DOPC ( $\gamma_{PS}=0.2$ ) which were fluctuating, quasispherical, i.e. with excess surface area. Fig. 5 shows a sequence of pictures of one vesicle after introducing  $\text{CaCl}_2$  in the experimental chamber. Snapshot A shows the quasispherical vesicle in a solution of 10 mM NaCl and glucose. The vesicle interior contains no glucose but sucrose, which enhances the optical contrast due to difference in the solutions refractive indices. The vesicle fluctuates strongly, indicating a large excess surface area (as compared to the area of a spherical vesicle of the same volume). An isotonic solution of 7 mM  $\text{CaCl}_2$  in glucose is then pumped into the chamber. After several minutes a homogeneous concentration of  $\text{CaCl}_2$  in the chamber is achieved and the calcium ions reach the vesicle membrane. The fluctuations decrease significantly and cease (Fig. 5B) leading

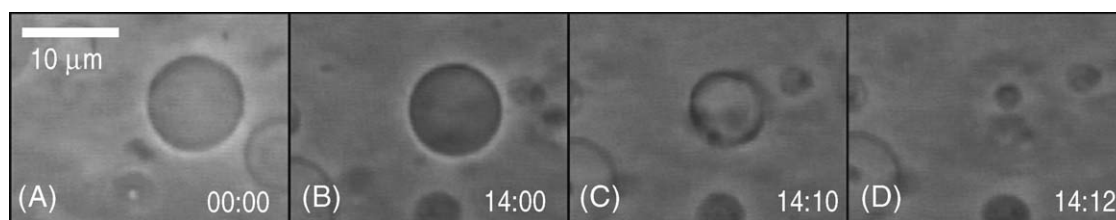


Fig. 5. A sequence of pictures of a giant DOPS:DOPC ( $\gamma_{PS}=0.2$ ) vesicle in 10 mM NaCl before and after injection of isoosmolar 7 mM  $\text{CaCl}_2$ . Time is relative and set to zero before injection as shown on each snapshot (min:s). (A) No  $\text{CaCl}_2$  is present; the vesicle strongly fluctuates. (B)  $\text{CaCl}_2$  solution has been injected and a significant decrease of fluctuations is observed. (C) The membrane appears thicker and the vesicle interior fades indicating leakage; the vesicle volume has also decreased. (D) The vesicle collapses and vanishes.



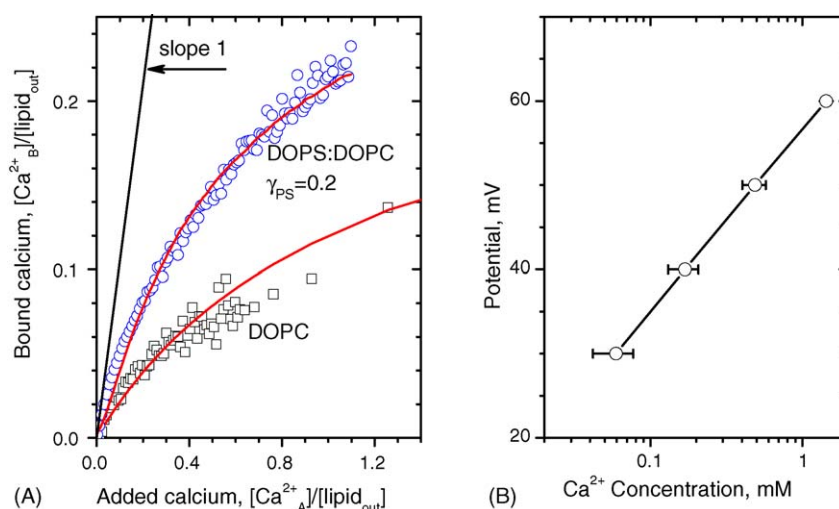


Fig. 6. (A) Binding isotherms of the titration of DOPS/DOPC ( $\gamma_{PS}=0.2$ ) and DOPC LUVs solution in 10 mM NaCl with 7 mM  $\text{CaCl}_2$ . The line indicated with “slope 1” represents the case of 100% binding. The concentration of bound ion  $[\text{Ca}_B^{2+}]$  was determined using a calibration curve before the measurement. The solid curve represents a fit with a 1:2 binding model [28]. (B) Calibration of the  $\text{Ca}^{2+}$  ISE. The error bar was determined from a calibration preceding and following the titration of the PS/PC mixture.

to a completely spherical vesicle with no excess area. The reason for the disappearing fluctuations can either be a stiffening of the membrane due to ion adsorption or an increase in the membrane tension. Soon afterwards, the vesicle appears to loose and exchange fluid with the exterior (Fig. 5C). A signature of the latter is that the internal contrast is lost which is due to leakage of sucrose solution (we remind that the vesicle appears dark initially due to the glucose/sucrose asymmetry of the solutions used). The hypothesis which best explains the observed dynamics is that the adsorption of the calcium ions causes condensation of the lipid molecules. An evidence for this is the seeming thickening of the vesicle membrane (Fig. 5C). The ion adsorption effectively results in tension. The latter approaches the lysis tension of lipid membranes leading to poration and leakage (Fig. 5C), and finally, membrane rupture and collapse (Fig. 5D). We can exclude osmotic effects as a cause for the vesicle rupturing because the osmolarity of the  $\text{CaCl}_2$  solution was carefully matched with that of the vesicle suspension.

From these observations we have to conclude that the binding of  $\text{Ca}^{2+}$  causes a decrease in the surface excess area of the vesicle. A straightforward comparison of calcium binding to giant vesicles (microscopic effects) and to LUVs (nano-scale effects) is difficult to deduce in terms of the effect of change in the area per lipid on the surface charge. The observations on giant vesicles cannot be precisely quantified because of the low optical resolution (about  $0.5\ \mu\text{m}$ ) which is far beyond the relevant scale for LUVs (tens of nanometers). However, with a certainty we can conclude that the observed microscopic effects can also be attributed to the tight binding of  $\text{Ca}^{2+}$  to the membrane coupled with dehydration of the lipid bilayer, leading to membrane tension.

#### 4.5. Estimating the amount of bound calcium with ISE

Coming back to the titration measurements, we want to estimate the amount of bound calcium,  $[\text{Ca}_B^{2+}]$ , with the addition

of  $\text{CaCl}_2$  to the LUV solution. Fitting the data directly would require usage of a model with many fitting parameters, e.g. the two molar enthalpies of binding of calcium to PC and PS, and the two equilibrium constants of these two processes. The large number of fitting parameters would make the fitting futile. In order to determine  $[\text{Ca}_B^{2+}]$  model-independently we use a  $\text{Ca}^{2+}$  ISE. The amount of bound  $\text{Ca}^{2+}$  as a function of molar ratio of  $[\text{Ca}_A^{2+}]$  to  $[\text{lipid}_{\text{out}}]$  for the titration of a 1.6 mM DOPC LUV with an 7 mM  $\text{CaCl}_2$  solution is plotted in Fig. 6A.  $[\text{Ca}_B^{2+}]$  was determined by subtracting the amount of free  $\text{Ca}^{2+}$  (measured by the electrode) from the added one. The line indicated with “slope 1” represents the case of 100% binding of the added  $\text{Ca}^{2+}$ . The experiment shows that  $\text{Ca}^{2+}$  indeed binds strongly to the zwitterionic PC headgroups. For very low calcium concentrations, almost all of the added ions bind to the vesicles while only a few remain free in the bulk solution. Additionally, binding of  $\text{Ca}^{2+}$  is not saturated even at  $[\text{Ca}_A^{2+}]$  to  $[\text{lipid}_{\text{out}}]$  ratios of 2 (data not shown), in very good agreement with the turbidity measurements. These results also affirm the interpretation of the ITC experiments that  $\text{Ca}^{2+}$  binding is not saturated at the end of the ITC experiment. Fitting this curve with the 1:2 binding model [20], we obtain a binding constant of  $250\ \text{M}^{-1}$ . This value is an order of magnitude larger than the value of  $20\ \text{M}^{-1}$ , now established in the literature. We remind that this value has been measured in presence of NaCl of concentration about 10 times higher than the present conditions, but in absence of NaCl the reported value for the binding constant is of the same order of magnitude [20].

In an attempt to explain this discrepancy, we question the possibility of interaction of the vesicles with the ion selective electrode leading to errors in the measured concentration of free  $\text{Ca}^{2+}$ . To probe for this, we performed calibrations of the ISE preceding and following the measurement and occasionally in the middle. The resulting averaged calibration curve is shown in Fig. 6B with the corresponding errorbars. Repeating several experiments revealed that the respective calibration curves differ

in their slope and intersection. This is indicative of an interaction of the lipids with the hydrophobic surfaces of the electrode membrane causing an additional change in the electrochemical potential. This finding is surprising as these problems were never discussed in the ISE measurements reported in literature.

The layer of lipid adsorbed on the electrode could lead to two effects: On one hand, the local concentration of calcium in the immediate vicinity of the electrode is elevated in comparison to the bulk solution because of the affinity of  $\text{Ca}^{2+}$  to PC, which would result in an apparent increase of the measured potential. This effect is expected to be further enhanced for measurements on PS/PC membranes. On the other hand, the lipid layer on the electrode surface also can prohibit the transport of ions across the electrode membrane. This would lead to the opposite effect, i.e. an apparent decrease in the measured electrochemical potential difference. The behavior of the calibration curve upon the addition of calcium, therefore, can change as a result of either of the two effects, and due to the two described opposing mechanisms, we cannot assess a priori whether the measured free  $\text{Ca}^{2+}$  concentration is an under- or overestimation of the “real” ion concentration. A fit of a binding isotherm determined with a calibration following the measurement indicates that apparently higher amount of  $\text{Ca}^{2+}$  are detected and yields an apparent binding constant of  $130 \text{ M}^{-1}$  (data not shown), which is significantly lower than the value of  $250 \text{ M}^{-1}$  determined with the primary calibration curve, but still a factor 6.5 higher than the literature value of  $20 \text{ M}^{-1}$ . However, it was already stated that direct comparison with data of other groups are not straightforward to perform, as a number of parameters influences the binding of  $\text{Ca}^{2+}$  to the membrane, such as the concentration of NaCl present in the system or the size (curvature) of the vesicles.

To our knowledge, the described effect of the vesicles on the calibration of an ion selective electrode has not yet been reported in the literature, but can be easily overseen. We, therefore, present these observations to alert other groups to take care that neutral and charged phospholipid membranes may seriously counterfeit the outcome of binding measurements using ion selective electrodes.

In the case of charged membranes, the ion concentration in the bulk solution monitored by ion selective electrodes is diminished both by electrostatic interactions, making the  $\text{Ca}^{2+}$  residing within the double layer near the membrane, and by actual  $\text{Ca}^{2+}$  binding to the headgroups of the phospholipid membrane. Consequently, the fraction of counterions immobilized in the diffusive part of the double layer could be erroneously ascribed to the bound fraction of ions. It is, therefore, essential to differentiate between intrinsic and apparent binding constants. While the former is given by the surface concentration of the binding ions, the latter is a function of the bulk ion concentration. Without additional information on the surface potential, ion selective membranes determine apparent binding affinities [7,34]. The interpretation of the results is further complicated by the presence of  $\text{Na}^+$ , which is also known to localize and bind to PS, although with a lower affinity [34,35]. Similar to the measurements on calcium binding to DOPC, the amount of bound  $\text{Ca}^{2+}$  to DOPS/DOPC LUVs was determined from a calibration curve preceding and following the measurement. Again, the interac-

tion of the vesicles with the ion selective membrane counterfeits the calibration curves. The amount of bound ions was calculated using the calibration before the titration. Fig. 6A shows the titration curve of 2.7 mM DOPS/DOPC ( $\gamma_{\text{PS}} = 0.2$ ) LUVs solution with small aliquots of 7 mM  $\text{CaCl}_2$  solution. For low  $\text{Ca}^{2+}$  concentrations, almost all of the added ions bind to the vesicles. Again, it is found that  $\text{Ca}^{2+}$  binds to the vesicles up to ratios far beyond the expected stoichiometric equivalence by charge of 0.5 (considering that each  $\text{Ca}^{2+}$  binds to two PS headgroup).  $\text{Ca}^{2+}$ -binding to the vesicles beyond the point of PS headgroup saturation and the fact that the binding heat approaches the value of  $\text{Ca}^{2+}$  binding to pure PC (as measured by ITC) strongly supports the picture given above that  $\text{Ca}^{2+}$  binds to both the PS and the PC headgroups. Fitting the binding isotherm of the ISE with the 1:2 binding model [28], we find an apparent binding constant of  $650 \text{ M}^{-1}$ . Considering the electrostatic enrichment within the double layer, this value is very similar to the value of the binding onto the pure DOPC vesicles. It is to be deduced that the presence of PS head groups favorably enriches calcium ions by electrostatic attraction nearby the membrane, but that actual binding onto the membrane is only of comparable strength.

## 5. Summary and conclusions

By combining a variety of techniques and systematic consideration of the data, it was shown that binding of calcium to zwitterionic and charged lipid bilayer membranes occurs spontaneously, but is an endothermic process, and therefore, entropy driven. It is assumed that the gain in entropy comes from a release of water molecules from the hydration shell of the ion as well as a dehydration of the lipid membrane. The latter is supported by the observation that  $\text{Ca}^{2+}$  binding leads to a tighter packing of the headgroups and the hydrocarbon chains. As a consequence, binding of the divalent cations to giant unilamellar vesicles has induced tension and rupture of the membrane.

Measurements with the ion selective electrode, although highly biased by hydrophobic interactions between the lipids and the electrode, showed that the binding of ions onto zwitterionic lipids and charged lipids occurs in an about comparable fashion. This was also supported by ITC measurements. The formal higher binding onto charged vesicles is potentially due to the electrostatic enrichment within the electrostatic double layer, but not due to the contact binding. Taking the higher endothermicity of the  $\text{Ca}^{2+}$ -binding onto charged membranes, it becomes obvious that the binding is not supported by electrostatics (which would be strictly exothermic), but on the contrary has to be supported by even a higher release of water molecules than for the zwitterionic membranes.

Qualitatively unaffected by the systematic errors of the ion selective electrode and supported by both turbidimetry and ITC, it was also quantitatively shown that  $\text{Ca}^{2+}$  binding is observed well beyond the point of electrostatic and even molar stoichiometry, that is the lipid membrane can bind more Ca-ions than it possesses lipid molecules. This is easily explained by a “binding-by dehydration”-model, but opposes any well-defined molecular model with defined binding pockets and coupled stoichiometries. The fact that membranes can bind and enrich even excesses

of ions is important for the processes of controlled biomineralization and makes them ideal spots of mineral nucleation due to local supersaturation.

Ongoing work in our group is devoted to a better understanding of ion binding onto neutral polymers and colloidal surfaces and a more detailed light scattering analysis of the  $\text{Ca}^{2+}$  binding onto LUVs.

## Acknowledgements

C.G.S. and R.D. acknowledge Karin A. Riske and Jeremy Pencer for helpful discussions.

## References

- [1] H.C. Lee, R. Aarhus, T.F. Walseth, *Science* 261 (1993) 352.
- [2] R. Lipowsky, E. Sackmann, *Structure and Dynamics of Membranes* (Handbook of Biological Physics), Elsevier, Amsterdam, 1995.
- [3] D. Papahadjopoulos, S. Nir, N. Düzgünes, *J. Bioenerg. Biomembr.* 22 (1990) 157.
- [4] A. Portis, C. Newton, W. Pangborn, D. Papahadjopoulos, *Biochemistry* 18 (1979) 780.
- [5] B. Alberts, A. Johnson, J. Lewis, M. Raff, K. Roberts, P. Walter, *Molecular Biology of the Cell*, Garland Science, New York, 2002.
- [6] A. McLaughlin, W.-K. Eng, G. Vaio, T. Wilson, S. McLaughlin, *J. Membr. Biol.* 76 (1983) 183.
- [7] S. McLaughlin, N. Mulrine, T. Gresalfi, G. Vaio, A. McLaughlin, *J. Gen. Physiol.* 77 (1981) 445.
- [8] M. Roux, M. Bloom, *Biochemistry* 29 (1990) 7077.
- [9] S. Nir, N. Duzgunes, J. Bentz, *J. Gen. Physiol.* 77 (1981) 445.
- [10] A. Lau, A. McLaughlin, S. McLaughlin, *Biochim. Biophys. Acta* 645 (1981) 279.
- [11] P. Macdonald, J. Seelig, *Biochemistry* 26 (1987) 1231.
- [12] G.W. Feigenson, *Biochemistry* 28 (1989) 1270.
- [13] J.R. Coorsen, R.P. Rand, *Biophys. J.* 68 (1995) 1009.
- [14] A. Averbakh, V.I. Lobyshev, *J. Biochem. Biophys. Methods* 45 (2000) 23.
- [15] R. Lehmann, J. Seelig, *Biochim. Biophys. Acta* 1189 (1994) 89.
- [16] K. Jacobson, D. Papahadjopoulos, *Biochemistry* 14 (1975) 152.
- [17] J. Silvius, J. Gagné, *Biochemistry* 23 (1984) 3241.
- [18] M. Roux, M. Bloom, *Biophys. J.* 60 (1991) 38.
- [19] H. Grasdalen, L. Eriksson, J. Westman, A. Ehrenberg, *Biochim. Biophys. Acta* 469 (1977) 151.
- [20] C. Altenbach, J. Seelig, *Biochemistry* 23 (1984) 3913.
- [21] D. Huster, K. Arnold, K. Gawrisch, *Biophys. J.* 78 (2000) 3011.
- [22] H. Akutsu, J. Seelig, *Biochemistry* 20 (1981) 7366.
- [23] S.J. Rehfeld, N. Düzgünes, C. Newton, D. Papahadjopoulos, D.J. Eatough, *FEBS Lett.* 123 (1981) 249.
- [24] H. Binder, O. Zschörnig, *Chem. Phys. Lipids* 115 (2002) 39.
- [25] R.C. MacDonald, R.I. MacDonald, B.Ph.M. Menco, K. Takeshita, N.K. Subbarao, L.-R. Hu, *Biochim. Biophys. Acta* 1061 (1991) 297.
- [26] D. Needham, E. Evans, *Biochemistry* 27 (1988) 8261.
- [27] R. Dimova, U. Seifert, B. Pouligny, S. Förster, H.-G. Döbereiner, *Eur. Phys. J. B* 7 (2002) 241.
- [28] J. Seelig, *Cell Biol. Int. Rep.* 14 (1990) 353.
- [29] K. Satoh, *Biochim. Biophys. Acta* 1239 (1995) 239.
- [30] R.A. Böckmann, H. Grubmüller, *Angew. Chem. Int. Ed.* 43 (2004) 1021.
- [31] A. McLaughlin, *Curr. Top. Membr. Transp.* 9 (1977) 71.
- [32] J.Y. Huang, J.E. Swanson, A.R.G. Dible, A.K. Hinderliter, G.W. Feigenson, *Biophys. J.* 2 (1993) 413.
- [33] S. Nebel, P. Ganz, J. Seelig, *Biochemistry* 36 (1997) 2853.
- [34] S. Nir, C. Newton, D. Papahadjopoulos, *Bioelectrochem. Bioenerg.* 5 (1978) 116.
- [35] R. Kurland, C. Newton, S. Nir, D. Papahadjopoulos, *Biochim. Biophys. Acta* 551 (1979) 137.
- [36] R. Ekerdt, D. Papahadjopoulos, *Proc. Natl. Acad. Sci.* 79 (1982) 2273.
- [37] G. Ceve, *Phospholipids Handbook*, Marcel Dekker Inc., New York, 1993.
- [38] P. Garidel, A. Blume, *Langmuir* 15 (1999) 5526.
- [39] C.G. Sinn, R. Dimova, M. Antonietti, *Macromolecules* 37 (2004) 3444.
- [40] D. Papahadjopoulos, *Biochim. Biophys. Acta* 163 (1968) 240.
- [41] T. Seimiya, S. Ohki, *Biochim. Biophys. Acta* 298 (1973) 546.
- [42] R.N.A.H. Lewis, B.D. Sykes, R.N. McElhaney, *Biochemistry* 27 (1988) 880.
- [43] J.L. Browning, J. Seelig, *Biochemistry* 19 (1980) 1262.
- [44] D. Bach, E. Wachtel, N. Borochoy, G. Senisterra, R.M. Epand, *Chem. Phys. Lipids* 63 (1992) 105.
- [45] C. Newton, W. Pangborn, S. Nir, D. Papahadjopoulos, *Biochim. Biophys. Acta* 506 (1978) 281.
- [46] S. Mann, *Biomineralization: Principles and Concepts in Bioinorganic Materials Chemistry*, Oxford University Press, Oxford, 2001.